JACS
JOURNAL OF THE AMERICAN CHEMICAL SOCIETY
Communication
pubs.acs.org/JACS

Redox Cycling on Recessed Ring-Disk Nanoelectrode Arrays in the Absence of Supporting Electrolyte

Chaoxiong Ma,[†] Nicholas M. Contento,[‡] and Paul W. Bohn*[,†,‡]

[†]Department of Chemistry and Biochemistry, University of Notre Dame, Notre Dame, Indiana 46556, United States
[‡]Department of Chemical and Biomolecular Engineering, University of Notre Dame, Notre Dame, Indiana 46556, United States

Supporting Information

ABSTRACT: In canonical electrochemical experiments, a high-concentration background electrolyte is used, carrying the vast majority of current between macroscopic electrodes, thus minimizing the contribution of electromigration transport of the redox-active species being studied. In contrast, here large current enhancements are achieved in the absence of supporting electrolyte during cyclic voltammetry at a recessed ring-disk nanoelectrode array (RRDE) by taking advantage of the redox cycling effect in combination with ion enrichment and an unshielded ion migration contribution to mass transport. Three distinct transport regimes are observed for the limiting current as a function of the concentration of redox species, $Ru(NH_3)_6^{2+/3+}$, revealed through the strong dependence of ion transport on ionic strength. Behavior at low analyte concentrations is especially interesting. In the absence of supporting electrolyte, ions accumulate in the nanopores, resulting in significantly increased current amplification compared to redox cycling in the presence of supporting electrolyte. Current enhancements as large as 100-fold arising from ion enrichment and ion migration effects add to the ~20-fold enhancement due to redox cycling, producing a total current amplification as large as 2000-fold compared to a single microelectrode of the same total area, making these RRDE arrays interesting for electrochemical processing and analysis.

The sensitivity of chip-based analytical devices using amperometric detection is governed, in part, by the mass transport of analytes to the electrode surface, which, in turn, dictates the magnitude of the measurable current.[1] Compared with macroelectrodes, microelectrodes exhibit enhanced mass transport and higher current density due to radial diffusion. The diffusion-controlled limiting current, I_{lim}, in voltammetry at a microdisk electrode with radius, r, is[2]

$$I_{lim} = 4nFDCr \quad (1)$$

where n is the number of electrons transferred, D is the diffusion coefficient, F is Faraday's constant, and C is the bulk concentration of the redox-active species. A dual electrode configuration operating with redox cycling (RC) represents an attractive geometry to enhance the measurable current and, thus, the sensitivity of amperometric detection.[3−5] In RC experiments, mass transport to the electrode surface does not depend directly on analyte diffusing from bulk solution, but rather on the regeneration and cycling of a redox couple between two closely spaced electrodes. The cycling of redox species multiplies the electron transfer reaction, resulting in current amplification that depends strongly on the spacing of the two electrodes. For example, the limiting current obtained for a thin-layer cell (TLC) geometry with radius of r and interelectrode distance of h is given by[4]

$$I_{lim} = \frac{\pi r^2 nFDC}{h} \quad (2)$$

Combining eqs 1 and 2 yields an amplification factor due to redox cycling (AF_{RC}) for a TLC compared to a single microelectrode of the same size,

$$AF_{RC} = \frac{\pi r}{4h} \quad (3)$$

As indicated by eq 3 and demonstrated previously, a TLC with electrode pairs can generate substantially amplified current as the interelectrode distance, h, shrinks to the nanoscale.[4,6] Although optimization of the electrode geometry by decreasing h and/or increasing r could produce a higher AF_{RC}, fabricating such devices remains challenging.

Equation 2 reveals that the I_{lim} in a given device relies directly on the diffusion coefficient, D, which governs the rate at which molecules move between two electrodes and the number of resulting redox events. However, eq 2 is valid for conditions where diffusion dominates, and electromigration contributes negligibly to mass transport, since the measurements are performed in the presence of a large concentration of supporting electrolyte (SE).[4] In contrast, at low ionic strength, ion migration can contribute significantly to mass transport.[7−9] This effect occurs because the Debye length, λ_D, depends on ionic strength, so at low ionic strength the electric field extends from the electrode surface into the bulk of solution, which can either promote or impede the movement of ions to the electrode surface.[10−12] The enrichment of $Ru(NH_3)_6^{3+/2+}$ in the negatively charged nanopores to maintain electroneutrality, a phenomenon that has been widely observed in nanopores and nanofluidic channels at low ionic strength, could also contribute to the observed current amplification.[13−15] Enhanced currents have been observed at low ionic strength on a single microelectrode, producing a several-fold increase in I_{lim} for the reduction of cationic species or oxidation of anionic species in the absence of SE.[7,8] In this study, we explore how migration

Received: March 8, 2014
Published: May 7, 2014

   dx.doi.org/10.1021/ja502052s | J. Am. Chem. Soc. 2014, 136, 7225−7228

effects, in combination with ion enrichment at nanopore-confined electrodes, might be further exploited to enhance mass transport in a dual electrode system exhibiting the RC effect, resulting in additional current amplification. Migration effects are expected to be larger in dual electrode systems,[16] since the electric field established across the two electrodes can drive the movement of ions, at least in one direction, speeding up the redox cycling events.

An array of recessed ring-disk electrodes (RRDE) with interelectrode distance, h = 150 nm, was fabricated, as shown in Figure 1, using a previously developed procedure.[5,17] Figure 2

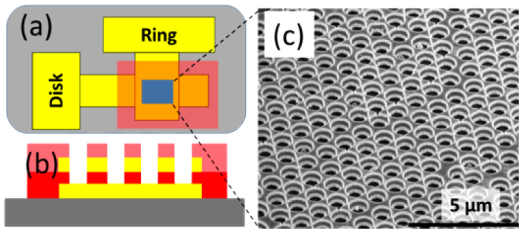

Figure 1. (a) Schematic diagram showing the macroscopic layout of the recessed ring-disk electrode array. (b) Cross section view of the array. The colors represent different layers: gray, glass slide; yellow, Au; red, SiN_x; and pink, SiO_2. (c) SEM image of the array at 50° tilt.

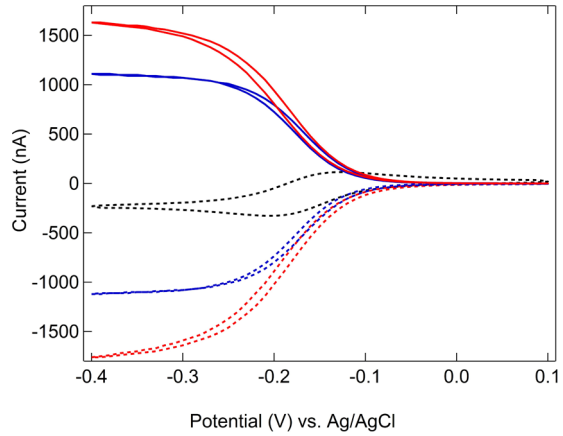

Figure 2. Cyclic voltammograms of 1 mM $Ru(NH_3)_6^{3+}$ on the RRDE array obtained by scanning the disk electrodes. Black curves: [KCl] = 0.1 M, ring electrodes floating, disk current multiplied by 5. Blue curves: [KCl] = 0.1 M, ring electrodes held at 0.1 V. Red curves: no SE, ring electrodes held at 0.1 V. Ring current (solid) and disk current (dashed). All potentials stated vs Ag/AgCl reference.

shows the voltammograms of 1 mM $Ru(NH_3)_6^{3+}$ in 0.1 M KCl solution measured at the disk electrodes on the RRDE array. The limiting current, I_{lim}, obtained on the disk electrodes with the ring electrodes left floating (non-RC mode) and held at 0.1 V (RC mode) were 57 and 1120 nA, respectively, yielding an AF_{RC} of ~20. This AF_{RC} is larger than the previously obtained AF_{RC} of ~10 obtained using $Fe(CN)_6^{3-/4-}$ on a RRDE array.[5] The higher collection efficiency is likely due to the larger RC number obtained with the larger electrode array used in this study (see Figure S1 and Table S1 in Supporting Information (SI)).

Cyclic voltammetry of 1 mM $Ru(NH_3)_6^{3+}$ without SE produces an ~50% increase in I_{lim}, viz. Figure 2. This additional current enhancement, AF_{ad}, is attributed to ion migration and nanopore-based ion enrichment and is quantified by

$$AF_{ad} = \frac{I_{lim,ase}}{I_{lim,se}} \quad (4)$$

where $I_{lim,ase}$ and $I_{lim,se}$ are the limiting currents obtained in RC mode in the absence and presence of SE, respectively. Both ion migration and ion enrichment effects, and the resulting AF_{ad}, depend strongly on the ionic strength, since it determines the extension of the electric field and the degree of electrostatic screening, as characterized by the Debye length, λ_D,[18]

$$\lambda_D = \frac{1}{\kappa} = \sqrt{\frac{\varepsilon_0 \varepsilon kT}{e_i^2 \sum C_i z_i^2}} \quad (5)$$

where ε and ε_0 are the relative electric permittivity of the solvent and permittivity of vacuum, respectively, k is the Boltzmann constant, T is the temperature, e is the elementary charge, and C_i and z_i are the concentration and charge of ion i, respectively. The inverse Debye length, κ, is introduced to characterize charge screening through the dimensionless group κh.

The results of investigations on different concentration of $Ru(NH_3)_6^{3+}$ (C_0) and λ_D, calculated using eq 5, are shown in Figure 3. In the presence of SE, $I_{lim,se}$ changes linearly with C_0,

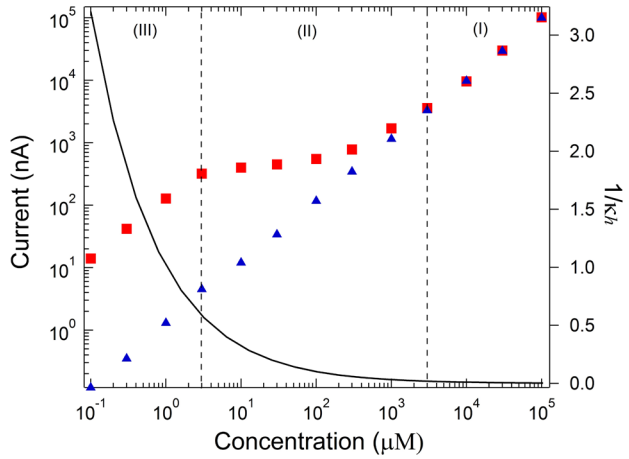

Figure 3. Limiting ring current of voltammograms of $Ru(NH_3)_6^{3+}$ as a function of concentration in 0.1 M KCl (blue) and in the absence of SE (red). Black curve: value of $1/\kappa h$ calculated at the corresponding $Ru(NH_3)_6^{3+}$ concentration in the absence of SE.

but in the absence of SE three distinct regions can be observed in the $I_{lim,ase}$ vs C_0 plot. In region I, there is negligible difference between $I_{lim,ase}$ and $I_{lim,se}$; in region II, $I_{lim,ase}$ plateaus; and in region III, it decreases again, but at substantially higher values than $I_{lim,se}$ at corresponding values of C_0.

Finite element calculations were performed to better understand the experimental observations and the role of migration in the observed current enhancement. The calculations account for the diffusion, migration and electrochemical reaction of ions at a single recessed ring-disk nanoelectrode pair. Calculated currents show a similar three-region dependence of $I_{lim,ase}$ on C_0, consistent with the value of λ_D changing with C_0 relative to the interelectrode (disk-to-ring) distance, h (150 nm) (Figure S4).

The observed and simulated behaviors can both be understood in terms of the dimensionless group, κh. At C_0 > 3 mM (region I, Figures 3 and S4), the migration contribution is negligible since $\kappa h \gg 1$; accordingly, the $I_{lim,ase}$ is nearly the

dx.doi.org/10.1021/ja502052s | J. Am. Chem. Soc. 2014, 136, 7225−7228

same as $I_{lim,se}$ and changes approximately linearly with C_0. At 3 μM < C_0 < 3 mM (region II), $I_{lim,ase}$ is larger than $I_{lim,se}$ and decreases only slightly with decreasing C_0, indicating larger AF_{ad} due to larger migration/ion enrichment contributions. In this region, $\kappa h \approx 1$. The decrease of κ (increase of λ_D) with decreasing C_0 leads to a larger migration contribution and faster movement of ions between the ring and disk electrodes. The mass transport that determines $I_{lim,ase}$ relies on both the number of ions within the interelectrode volume and their rate of movement between ring and disk electrodes. Hence, an increase in the migration component and ion enrichment produced upon decreasing C_0 partly counteracts the effect of reduced ion concentration in bulk solution, resulting in the relatively flat $I_{lim,ase}$ in region II. In region III (C_0 < 3 μM), $I_{lim,ase}$ again exhibits a linear response with C_0. Since κh < 1 throughout region III, the electric field is relatively concentration independent. Thus, the migration contribution to ion transport becomes relatively independent of C_0 in this region. In addition, at low ion concentration, competitive ions, such as H^+ due to dissolution of CO_2 and K^+ leaking from the reference electrode, could be large enough to perturb the ion enrichment, thereby decreasing the accumulation of $Ru(NH_3)_6^{3+/2+}$. As a result, $I_{lim,ase}$ responds to the concentration of redox species.

The typical AF_{ad} obtained in region III is around 100, which is much higher than the values reported previously for a single electrode[7,8] and an ultrathin-layer cell.[16] This difference can be attributed to a large migration effect due to a nanoscale value of h and ion enrichment in the nanopore geometry. At small h, the electric field established between the positively charged ring and negatively charged disk electrodes speeds transport of $Ru(NH_3)_6^{3+}$ ions to the disk electrodes. The same electric field obviously impedes $Ru(NH_3)_6^{2+}$ ions moving toward the ring electrodes, but to a smaller degree. Clearly, the mass transport of ions to the disk electrodes is the crucial limiting factor for the redox cycling reaction on the array. This observation is supported by the smaller collection efficiency obtained on disk electrodes than on ring electrodes demonstrated previously[5] and reproduced here, viz. Table S1. Another key factor contributing to a larger AF_{ad} obtained at lower C_0 is the accumulation of $Ru(NH_3)_6^{3+/2+}$ ions in the nanopores, as indicated by increasing I_{lim} with the scan number in CV measurement of 1 μM $Ru(NH_3)_6^{3+}$ solution in the absence of SE, viz. Figure 4. This phenomenon occurs only in the absence of SE and is more prominent at low C_0 (see SI), thus leading to a higher AF_{ad} at lower C_0.

The combination of an $AF_{ad} \approx 100$ and $AF_{RC} \approx 20$ gives a total amplification $AF_{total} \approx 2000$, compared to measurements on a single electrode of the same total area in the presence of SE. We note that the migration effect, ion enrichment, and their resulting AF_{ad} rely strongly on the charge of the ionic species, which has been demonstrated previously.[7,8,13] Indeed, AF_{ad} is much smaller for measurement of neutral ferrocenemethanol compared to $Ru(NH_3)_6^{3+}$ on the RRDE array (data not shown). In future applications, this charge dependence of AF_{ad} could be used to improve the selectivity of voltammetric measurements to distinguish between species in different charge states.

In conclusion, we have demonstrated that ion enrichment and the ion migration contribution to mass transport in a nanoscale RRDE array are enhanced in the absence of SE, resulting in a current amplification as large as 2000-fold. Three distinct regions were observed in the dependence of I_{lim} on analyte concentration in the absence of SE, these being largely determined by the dimensionless factor κh, which dictates the degree of overlap between the electric double layers of the nanopores and that of adjacent electrodes and thus the degree to which ion enrichment and ion migration enhance current.

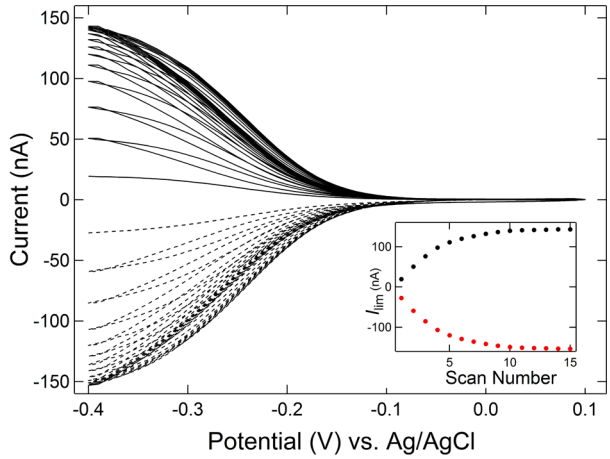

Figure 4. Repeated cyclic voltammograms of 1 μM $Ru(NH_3)_6^{3+}$ scanned at the disk electrodes of an RRDE array, with ring electrodes at 0.1 V, in the absence of SE: ring current (solid) and disk current (dashed). (Inset) Variation of limiting current with the scan number: ring current (black) and disk current (red).

■ ASSOCIATED CONTENT

Supporting Information

Discussion of the experimental setup, collection efficiency and current amplification of the array, variation of limiting ring current with scan number, and finite element calculations. This material is available free of charge via the Internet at http://pubs.acs.org.

■ AUTHOR INFORMATION

Corresponding Author

pbohn@nd.edu

Notes

The authors declare no competing financial interest.

■ ACKNOWLEDGMENTS

This work was supported by the National Science Foundation, grant 1111739 (C.M.), and by the Department of Energy Basic Energy Sciences, grant DE FG02 07ER15851 (N.M.C.).

■ REFERENCES

(1) Wang, J. *Talanta* **2002**, *56*, 223.
(2) Saito, Y. *Rev. Polarogr.* **1968**, *15*, 177.
(3) Niwa, O.; Morita, M.; Tabei, H. *Anal. Chem.* **1990**, *62*, 447.
(4) Wolfrum, B.; Zevenbergen, M.; Lemay, S. *Anal. Chem.* **2008**, *80*, 972.
(5) Ma, C.; Contento, N. M.; Gibson, L. R.; Bohn, P. W. *ACS Nano* **2013**, *7*, 5483.
(6) Zevenbergen, M. A. G.; Wolfrum, B. L.; Goluch, E. D.; Singh, P. S.; Lemay, S. G. *J. Am. Chem. Soc.* **2009**, *131*, 11471.
(7) Amatore, C.; Fosset, B.; Bartelt, J.; Deakin, M. R.; Wightman, R. M. *J. Electroanal. Chem. Interfacial Electrochem.* **1988**, *256*, 255.
(8) Oldham, K. B. *J. Electroanal. Chem. Interfacial Electrochem.* **1988**, *250*, 1.
(9) Cooper, J. B.; Bond, A. M.; Oldham, K. B. *J. Electroanal. Chem.* **1992**, *331*, 877.
(10) Zhang, Y.; Zhang, B.; White, H. S. *J. Phys. Chem. B* **2006**, *110*, 1768.

(11) Belding, S. R.; Compton, R. G. *J. Electroanal. Chem.* **2012**, *683*, 1.
(12) Bund, A.; Kubeil, C. *Faraday Discuss.* **2013**, *164*, 339.
(13) Schoch, R. B.; Renaud, P. *Appl. Phys. Lett.* **2005**, *86*, 253111.
(14) Stein, D.; Kruithof, M.; Dekker, C. *Phys. Rev. Lett.* **2004**, *93*, 035901.
(15) Zhou, K.; Kovarik, M. L.; Jacobson, S. C. *J. Am. Chem. Soc.* **2008**, *130*, 8614.
(16) White, H. S.; Xiong, J. *Book of Abstracts*, 11th Spring Meeting of the International Society of Electrochemistry, May 23−25, 2012, Georgetown University; International Society of Electrochemistry: Lausanne, Switzerland, 2012; p 64.
(17) Ma, C.; Contento, N. M.; Gibson, L. R.; Bohn, P. W. *Anal. Chem.* **2013**, *85*, 9882.
(18) Myers, D. *Surfaces, interfaces, and colloids*; Wiley-VCH: New York, 1999.